RSC Advances

PAPER

View Article Online
View Journal | View Issue



Cite this: *RSC Adv.*, 2020, **10**, 37596

# Converting waste textiles into highly effective sorbent materials†

Bijan Nasri-Nasrabadi and Nolene Byrne *

Received 25th May 2020
Accepted 24th August 2020

DOI: 10.1039/d0ra04616g

rsc.li/rsc-advances

Activated carbon fibres with a tubular structure and exfoliated surface were produced utilizing cotton textile waste as the precursor. The synthesized carbon fibres were freeze dried resulting in a tubular structure and large pore size distribution. The absorption properties against various oils and organic solvents were accessed, these fibres showed some of the highest absorption capabilities reported for cellulose based carbons, in particular for olive oil, gasoline and chloroform.



## Introduction

A significant amount of textile waste is disposed of in landfill; textile waste accounts for 10–20% of landfill depending on the country.[1,2] As such, new approaches for recycling and utilizing waste textiles are under constant development.[3,4] One potential solution is the use of cotton based textile waste as a precursor for carbon materials. These materials have applications in areas such as energy storage,[5,6] catalyst supports,[7,8] and filtration.[9,10] In particular for filtration, the low density and inherent hydrophobic nature of carbon substrates make them suitable to remove oil and organic solvents from wastewater.[11,12] Carbon substrates can be obtained from either synthesized or natural polymer based materials. However, harmful and expensive starting materials are the key issues associated with the carbon substrates obtained from the synthesized precursors.[13] In contrast, waste cotton is an abundant, sustainable and nontoxic resource as cotton is predominately a cellulosic polymer. To date a range of different cellulosic based precursors have been used as absorption substrates and the performance is generally very good owing to high surface area and porosity.[14–17] In this study, we report a facile route to produce carbon fibres from waste cotton textile garments; the fibres show significantly higher absorption capabilities than previous reports, due to a tubular structure and exfoliated surface created by combining a freeze drying and $CO_2$ activation. Regenerated cellulose fibres are wet spun using cotton waste and a binary ionic liquid solvent, complete experimental details has been previously published.[4,18] The fibres are either air dried as is standard method for producing regenerated cellulose fibres or freeze dried prior to carbonization. Carbonization was achieved by heating the fibres in a nitrogen atmosphere at 5 °C $min^{-1}$ up to 1100 °C and held for 1 hour.

Fig. 1 shows the SEM image of fibre before and after carbonization for both air and freeze dried approaches. The air dried regenerated cellulose fibre exhibits a smooth surface area with a solid and highly packed cross-section as is typical,[19,20] the diameter is in the range of 22 ± 3 μm (Fig. 1a). Fig. 1b is the SEM image of the freeze dried fibre (FDF) a different morphology is observed here when compared to the air dried fibre. The FDF shows an exfoliated morphology with microchannels, in the range of 0.5 to 2 μm on the surface. It can also be seen that the freeze drying has resulted in a tubular cross section, with an inner diameter range of 15 ± 3 μm and an outer diameter in the range of 22 ± 3 μm. Fig. 1c shows the air dried sample after carbonization (ADCF). A solid cross section and a smooth surface morphology (Fig. 1c) remains, however a reduction in the diameter has resulted, the diameter has reduced to 5 ± 3 μm. Fig. 2d shows the carbonized freeze dried sample, the exfoliated surface remains as does the tubular structure, with an inner diameter of 12 ± 3 μm and an outer diameter of 17 ± 3 μm. In order to further increase the surface area and porosity, we subjected the freeze dried fibres to $CO_2$ activation, $CO_2$ activation was achieved by exposing the carbonized fibres to $CO_2$ flow for 1 hour at 800 °C. Fig. 2e is the $CO_2$ activated freeze dried carbon fibres (AFDCF). The outer surface of the $CO_2$ activated fibres appears very similar to the freeze dried sample however, new pores in the dimension range less than 1 μm appear on the inner surface of the fibres (Fig. S1†). During the activation, $CO_2$ reacts with carbon atoms *via* $C + CO_2 \rightarrow CO + C(O)$, where the first product is carbon monoxide gas and the second product is various oxygen complexes which develop on the carbon substrate. The above reaction removes delicate carbon atoms from the substrate *via* the conversion of carbon to carbon monoxide gas (CO).[21,22] The generated CO creates new pores on the fibres inner surface.

Table 1 lists the pore characteristics of the fibres before and after carbonization, obtained from $N_2$ absorption. As expected,

*Institute for Frontier Materials, Deakin University, Geelong, Victoria 3216, Australia. E-mail: nolene.byrne@deakin.edu.au*

† Electronic supplementary information (ESI) available. See DOI: 10.1039/d0ra04616g

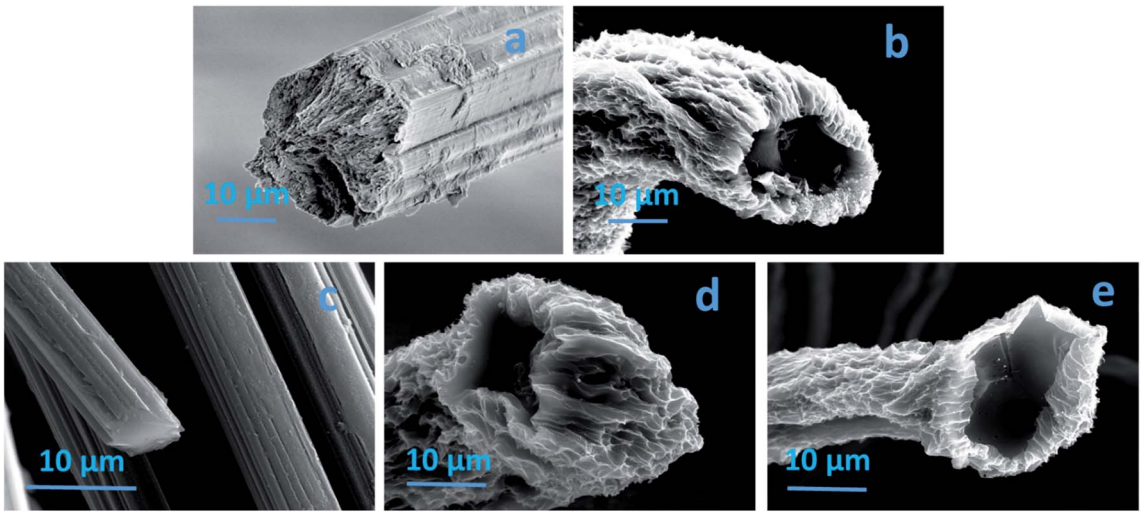


Fig. 1 (a) The SEM image of the air dried fibre (ADF), (b) freeze dried fibre (FDF), (c) air dried carbon fibre (ADCF), (d) freeze dried carbon fibre (FDCF), and (e) $CO_2$ activated freeze dried carbon fibre (AFDCF).

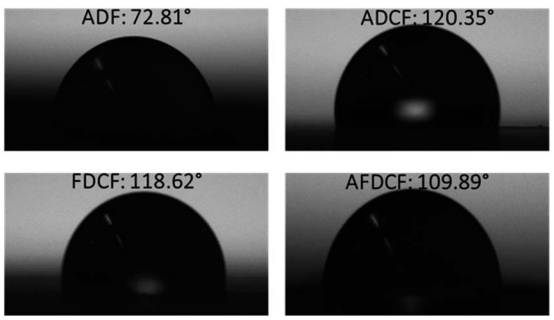


Fig. 2 The water contact angle measurement of air dried fibre (ADF), air dried carbon fibre (ADCF), freeze dried carbon fibre (FDCF), and $CO_2$ activated freeze dried carbon fibres (AFDCF).

the freeze dried fibres (FDF) show an overall higher pore volume and surface area compared with the air dried fibres (ADF). The FDF displays a cumulative pore volume and surface area of 13.51 $cm^3\ g^{-1}$ and 89 $m^2\ g^{-1}$, while the ADF sample displays a cumulative pore volume and surface area of 0.02 $cm^3\ g^{-1}$ and 2 $m^2\ g^{-1}$. Carbonization of the fibres resulted in the generation of pores in the meso and micropore range for both ADF and FDF fibres. This is due to the removal of the non-carbon elements. In the case of the $CO_2$ activated fibre, larger pores in the range of macro are present. As the results show the macropores volume of the FDCF increased from 12.37 $cm^3\ g^{-1}$ to 25.74 $cm^3\ g^{-1}$ with $CO_2$ activation. We also observed a significant increase of the surface area from 197 $m^2\ g^{-1}$ for the FDCF to 312 $m^2\ g^{-1}$ for the $CO_2$ activated FDCF. As such the $CO_2$ activation applied here, produces fibres with a greater pore size distribution.

The fibres hydrophobicity was measured, which is a key parameter to determine material capacity and performance to absorb organic solvents and spilled oils. Fig. 2 is the contact angle values before and after carbonization. Regenerated cellulose fibres are highly hydrophilic, in general, here the water contact angle was measured to be 72.81°, an increase in hydrophobicity results from carbonization. The carbonized air dried and freeze dried samples showed almost similar contact angle values of 120.35° and 119.62° respectively. After $CO_2$ activation, however, we found a slight decrease in the contact angle, the $CO_2$ activated sample (AFDCF) has a water contact angle of 109.89°, which is around 10 degree lower than the value range of other the two carbonized fibres. This decrease can be due to the generation of new oxygen complexes on the carbon fibres surface after the $CO_2$ activation.

ATR-FTIR analyse shows the change in the surface groups for the regenerated cellulose and carbonized cellulose fibres. The freeze dried cellulose fibre reveals characteristic peaks of hydrophilic functional groups (Fig. 3). The absorption peak at 1065 $cm^{-1}$ ascribes to the skeletal vibration of C–O–C groups.

Table 1 Pore properties of the fibres before and after carbonization

| Sample | Surface area, $m^2\ g^{-1}$ | Pore volume, $cm^3\ g^{-1}$ | Micropores volume, $cm^3\ g^{-1}$ | Mesopores volume, $cm^3\ g^{-1}$ | Macropores volume, $cm^3\ g^{-1}$ |
|---|---|---|---|---|---|
| ADF | 2 | 0.02 | 0.02 | 0 | 0 |
| FDF | 89 | 13.51 | 0.04 | 0.12 | 13.35 |
| ADCF | 72 | 0.09 | 0.05 | 0.04 | 0 |
| FDCF | 197 | 12.60 | 0.08 | 0.15 | 12.37 |
| AFDCF | 312 | 25.96 | 0.11 | 0.10 | 25.74 |

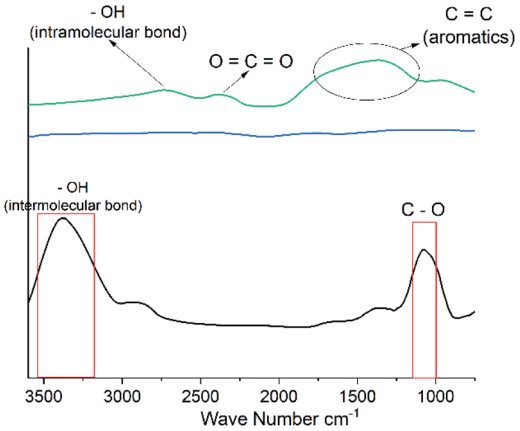


Fig. 3 The ATR-FTIR spectra of the freeze dried cellulose fibre (FDF) (black), freeze dried carbon fibre (FDCF) (blue), and $CO_2$ activated freeze dried carbon fibres (AFDCF) (green).

The broad peak between 3100 $cm^{-1}$ and 3600 $cm^{-1}$ ascribed to stretching of –OH groups. It should be stated that both the freeze dried and air dried cellulose fibres showed similar spectrums. After carbonization, as the FTIR results show these functional groups have disappeared, as is expected for carbonized materials and explains the change from hydrophilic to hydrophobic substrates. For the $CO_2$ activated sample, two weak absorption peaks in the range 3200–2700 $cm^{-1}$ and around 2350 $cm^{-1}$ are observed, this likely ascribe to the –OH intramolecular bonds and O=C=O groups. These new absorption peaks correlate to the formation of new oxygen complexes after $CO_2$ activation and thus the lowering of the contact angle.

In order to quantify the absorption performance, the weight gain is defined as the weight of the uptake liquid per the dried fibres weight. Fig. 4 shows the weight gain values of the three different carbon fibres, air dried (ADCF), freeze dried (FDCF) and $CO_2$ activated (AFDCF) for heptane, ethanol, chloroform, gasoline, and olive oil. Based on the results, we found that in general the FDCF displayed a higher absorbance capability than the ADCF, which correlates to the exfoliated surface morphology and the tubular structure. As can be seen, the FDCF shows around 71%, 91%, 41%, 41%, and 34% higher weight gain, when compared to the ADCF (for ethanol, heptane, chloroform, gasoline, and olive oil respectively). With $CO_2$ activation, we observed a significant enhancement in the weight again performance for all solutes tested. The $CO_2$ activated fibre demonstrate an absorption capacity range of 75–175 g $g^{-1}$, which is higher than that of sorbents from other lignocellulosic sources such as carbon aerogels from winter melon (25–50 g $g^{-1}$),[23] carbon nanofiber hydrogel/aerogels (45–65 g $g^{-1}$),[24] carbon fibre aerogels derived from bamboo (40–75 g $g^{-1}$),[15] hollow carbon fibres sponges from crude catkins (75–140 g $g^{-1}$),[25] and carbon fibre aerogel made from raw cotton (50–110 g $g^{-1}$)[11] for similar solutes. The increase in the absorption capacity of the activated sample reported here is likely due to the generation of additional macropores, upon activation.

The recoverability of the sorbent and the recyclability of the absorbed chemical are key factors in developing a cost effective water clean-up processes. Generally, an absorbed chemical is extracted *via* either distillation for useful chemicals with low boiling points, squeezing for useful chemicals with high boiling points or combustion for useless and flammable chemicals. Here the recoverability of the sorbent after combustion and also the recyclability of the solutes *via* an absorption/distillation process was accessed using ethanol and gasoline. Direct consumption in air is used to test the absorption/consumption recoverability of the $CO_2$ activated freeze dried carbon fibre (AFDCF). After five absorption/consumption cycles, for ethanol and gasoline, we observed 96% and 90% respectively of their weight gain capacity in comparison to the first cycle Fig. 5a shows the 5 absorption/consumption cycles for ethanol and the corresponding gasoline data is in the ESI Fig. S2a.† The higher

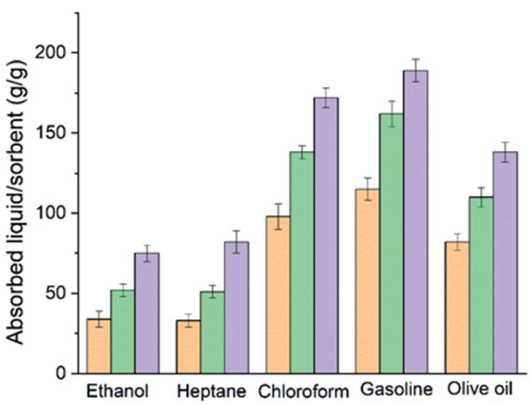


Fig. 4 Weight gain values for different solutes, where orange is for air dried carbon fibres (ADCF), green is for freeze dried carbon fibres (FDCF) and purple for $CO_2$ activated freeze dried carbon fibre (AFDCF).

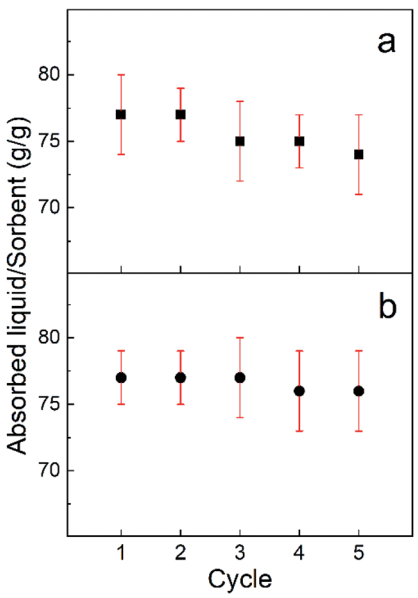


Fig. 5 (a) The absorption/combustion and (b) the absorption/distillation recyclability of the $CO_2$ activated freeze dried carbon fibres with ethanol.

decrease in the absorption capacity of the carbon fibres for gasoline is most likely due to the deposition of residues within the porous structure and on the surface of the carbon fibres after combustion.[26]

We also employed distillation to recover the carbon fibres and harvest the chemical. Ethanol with a boiling point of around 78 °C and gasoline with a boiling point of around 200 °C were used to demonstrate recyclability of the absorbed solute and the recoverability of the sorbent after each absorption/distillation cycle. Fig. 5b shows the trend of absorption/distillation cycles for ethanol, repeated for five times. We found that, the AFDCF can almost fully recover its absorption capacity with no noticeable change of the sorbent mass after each cycle. This suggests the self-supporting microstructure of the porous carbon fibres and allows the sorbent to preserve its saturated capacity with a repeatable performance. Regarding the gasoline, we again found a decline in the absorption capacity of the fibres after each cycle. As Fig. S2b† shows the saturated capacity of the carbon fibres after the 2th, 3rd, 4th, and 5th cycles was 91%, 90%, 84%, and 82% compared to cycle 1.

## Conclusions

In this study we developed a facile method to produce tubular carbon fibres utilizing cotton waste textile as the precursor. The obtained fibres exhibited an exfoliated surface area. We found that $CO_2$ activation enhanced the surface area and resulted in a broader pore size distribution. The absorption capacity of these new fibres was examined and they showed extremely excellent absorption ability, some the highest absorption values reported to date for cellulosic based carbon materials.

## Conflicts of interest

There are no conflicts to declare.

## References

1 Y. Wang, *Waste Biomass Valorization*, 2010, **1**, 135–143.
2 G. Sandin and G. M. Peters, *J. Cleaner Prod.*, 2018, **184**, 353–365.
3 B. Zeng, X. Wang and N. Byrne, *Carbohydr. Polym.*, 2019, **205**, 1–7.
4 Y. Ma, B. Zeng, X. Wang and N. Byrne, *ACS Sustainable Chem. Eng.*, 2019, **7**, 11937–11943.
5 L. Li, F. Lu, C. Wang, F. Zhang, W. Liang, S. Kuga, Z. Dong, Y. Zhao, Y. Huang and M. Wu, *J. Mater. Chem. A*, 2018, **6**, 24468–24478.
6 Y. Cui, W. Liu, Y. Lyu, Y. Zhang, H. Wang, Y. Liu and D. Li, *J. Mater. Chem. A*, 2018, **6**, 18276–18285.
7 A. M. ElKhatat and S. A. Al-Muhtaseb, *Adv. Mater.*, 2011, **23**, 2887–2903.
8 A. C. Pierre and G. M. Pajonk, *Chem. Rev.*, 2002, **102**, 4243–4266.
9 Q. Zuo, Y. Zhang, H. Zheng, P. Zhang, H. Yang, J. Yu, J. Tang, Y. Zheng and J. Mai, *Chem. Eng. J.*, 2019, **365**, 175–182.
10 K. K. Shimabuku, T. L. Zearley, K. S. Dowdell and R. S. Summers, *Environ. Sci.: Water Res. Technol.*, 2019, **5**, 849–860.
11 H. Bi, Z. Yin, X. Cao, X. Xie, C. Tan, X. Huang, B. Chen, F. Chen, Q. Yang and X. Bu, *Adv. Mater.*, 2013, **25**, 5916–5921.
12 A. Saini, P. H. Maheshwari, S. S. Tripathy, S. Waseem and S. Dhakate, *Journal of Water Process Engineering*, 2020, **34**, 101136.
13 Z. Y. Wu, C. Li, H. W. Liang, J. F. Chen and S. H. Yu, *Angew. Chem., Int. Ed.*, 2013, **52**, 2925–2929.
14 K. Hina, H. Zou, W. Qian, D. Zuo and C. Yi, *Cellulose*, 2018, **25**, 607–617.
15 S. Yang, L. Chen, L. Mu, B. Hao and P.-C. Ma, *RSC Adv.*, 2015, **5**, 38470–38478.
16 H. Voisin, L. Bergström, P. Liu and A. P. Mathew, *Nanomaterials*, 2017, **7**, 57.
17 N. El Badawi, A. R. Ramadan, A. M. Esawi and M. El-Morsi, *Desalination*, 2014, **344**, 79–85.
18 B. Nasri-Nasrabadi, X. Wang and N. Byrne, *J. Text. Inst.*, 2020, 1–10.
19 Y. Ma, B. Nasri-Nasrabadi, X. You, X. Wang, T. J. Rainey and N. Byrne, *J. Nat. Fibers*, 2020, 1–13.
20 W. P. F. Neto, J.-L. Putaux, M. Mariano, Y. Ogawa, H. Otaguro, D. Pasquini and A. Dufresne, *RSC Adv.*, 2016, **6**, 76017–76027.
21 G. Zu, J. Shen, L. Zou, F. Wang, X. Wang, Y. Zhang and X. Yao, *Carbon*, 2016, **99**, 203–211.
22 Q. Hu and M.-S. Kim, *Carbon Lett.*, 2008, **9**, 298–302.
23 Y.-Q. Li, Y. A. Samad, K. Polychronopoulou, S. M. Alhassan and K. Liao, *ACS Sustainable Chem. Eng.*, 2014, **2**, 1492–1497.
24 H. W. Liang, Q. F. Guan, L. F. Chen, Z. Zhu, W. J. Zhang and S. H. Yu, *Angew. Chem., Int. Ed.*, 2012, **51**, 5101–5105.
25 L. Zang, Z. Bu, L. Sun and Y. Zhang, *RSC Adv.*, 2016, **6**, 48715–48719.
26 K.-W. Youm and S.-J. Kim, *Journal of the Korea Society For Power System Engineering*, 2014, **18**, 11–15.